Structural relaxation and nonexponential kinetics of CO-binding to horse myoglobin

Multiple flash photolysis experiments

F. Post, W. Doster, G. Karvounis, and M. Settles

Technische Universität München, Physik-Department E13, D-8046 Garching, Germany

ABSTRACT   The geminate recombination kinetics of CO-myoglobin strongly deviates from single exponential behavior in contrast to what is expected for unimolecular reactions (1). At low temperatures, this result was attributed to slowly exchanging conformational states which differ substantially in barrier height for ligand binding. Above 160 K the kinetics apparently slow down with temperature increase. Agmon and Hopfield (2) explain this result in terms of structural relaxation perpendicular to the reaction coordinate, which enhances the activation energy. In their model, structural relaxation homogenizes the kinetic response. Recently, Steinbach et al. (3) proposed a relaxation model which conserves the kinetic inhomogeneity. Below we test these conjectures by single and multiple excitation experiments. This method allows for discrimination between parallel (inhomogeneous) and sequential (homogeneous) kinetic schemes. The kinetic anomaly above 160 K is shown to result from a homogeneous, structurally relaxed intermediate. However a second anomaly is found above 210 K concerning the inhomogeneous phase which may indicate either a shift in activation energy or entropy.

1 INTRODUCTION

Nonexponential relaxation is a prominent feature of many complex structured systems including biomolecules. Explanations of its molecular origin can be classified by two extreme situations: (a) structural inhomogeneity in the sample causes a distribution of relaxation rates. The relaxation function appears as a superposition of independent exponential processes. Thus each particular molecule can assume only two states. (b) For a multiplicity of internal states, relaxation may involve a sequence of intermediates which leads to nonexponential kinetics if the transition rates are comparable. The system now appears homogeneous because the individual molecules cannot be distinguished by their kinetic behavior. Case (b) frequently applies to multistep reactions in proteins such as the photocycle in bacteriorhodopsin. Case (a) may arise for structure dependent reactions which occur on time scales faster than typical mixing times of structural states. The distinction between homogeneous and inhomogeneous situations may determine whether a conformational change merely represents a small shift, which is accessible to equilibrium fluctuations, or whether it involves a high energy pertubation of the equilibrium structure. This question lies at the center of a controversy concerning the interpretation of structural relaxation effects on the kinetics of ligand binding to myoglobin (1–3).

In 1975 Austin et al. (1) published a series of flash photolysis experiments on carboxy-myoglobin (sperm whale) which were carried out within a wide range of time and temperature. Besides the well known bimolecular process they observed internal or geminate recombination. The most surprising feature of the geminate phase was its nonexponential kinetic shape whose de-

scription required a rate distribution extending over several decades in frequency. This result is in contrast to the exponential kinetics expected of elementary unimolecular reactions. Assuming the Arrhenius law, it was possible to account for the data in terms of a temperature invariant distribution of activation enthalpies $g(H_0)$. The survival fraction of the geminate pair $N(t)$ is then written as a parallel superposition of exponential processes:

$$N(t) = \int_0^\infty dH_0 \cdot g(H_0) \cdot \exp(-k(H_0, T) \cdot t), \qquad (1)$$

where $k(H_0, T)$ is given by the Arrhenius law. Eq. 1 suggests that the protein molecules can assume a large number of slowly exchanging structural states which differ substantially in barrier height for rebinding.

This description holds up to 160 K. At higher temperatures the kinetics apparently slow down at long times and deviate from Eq. 1. Finally, above 200 K a bimolecular process, depending on the ligand concentration in the solvent, terminates the kinetics at long times. The slowing down above 160 K was initially attributed to a ligand displacement out of the heme pocket and rebinding from the protein matrix (4). Agmon and Hopfield (2) in contrast proposed to relate this effect to the relaxation of a structural coordinate towards a global minimum, which increases the apparent activation energy for rebinding. In addition to a shift in activation energy this model also predicts a collapse of the distribution or exponential kinetics at long times, since relaxation and configurational mixing occur simultaneously. Thus:

$$g(H_0) \xrightarrow{r_c} \delta(H - H_f). \qquad (2)$$

H_f refers to the final energy of the relaxed structure and $\delta(x)$ denotes the delta-function. To derive the kinetics, we use the concept of a time-dependent activation energy (3) which simplifies the treatment of reference 2 significantly:

$$H(t) = H_f + (H_0 - H_f) \cdot \exp(-(t/\tau_c)^\beta). \qquad (3)$$

The stretched exponential accounts for structural reorganization, which is assumed to be uniform for all states specified by H_0. Consequently, one has to introduce a time-dependent Arrhenius law and a configurationally (H_0) averaged survival fraction of the geminate pair:

$$k(t) = A \cdot \exp(-H(t)/R \cdot T)$$

$$N(t) = \int_0^\infty dH_0 \cdot g(H_0) \cdot \exp\left(-\int_0^t k(t') \, dt'\right). \qquad (4)$$

Using only the low temperature distribution $g(H_0)$ as input, Agmon and Hopfield (2) predict $H_f \approx 32$ kJ/mol. This value is not compatible with the activation energy (12 kJ/mol) of the overall binding process at physiological temperatures, where the barrier at the heme should be rate limiting. Srajer et al. (5) proposed to identify the structural coordinate with the out-of-plane position of the heme iron. Allowing for partial relaxation already at low temperatures they obtained $H_f \approx$ 18 kJ/mol. A similar value was derived by establishing a correlation between the peak position of the inhomogeneous charge transfer band at 760 nm and kinetic data: In a series of kinetic hole burning experiments (3) Frauenfelder and collaborators confirmed the idea of structural relaxation as the origin of the kinetic slowing down. However, to be compatible with spectroscopic data and in view of the persistence of nonexponential kinetics in the relaxation regime, they propose an inhomogeneous relaxation model:

$$g(H_0) \xrightarrow{\tau_c} g(H_0 + \Delta H). \qquad (5)$$

Thus each structure with initial activation energy H_0 is linked to a state in the relaxed structure by a fixed energy shift ΔH:

$$H(t) = H_0 + \Delta H \cdot (1 - \exp(-(t/\tau_c)^\beta)). \qquad (6)$$

The kinetics is calculated according to Eq. 4. This implies that the equilibration of substates is slow compared to the relaxation.

In the following, we test these models (Eqs. 3–6) for horse myoglobin using single and multiple flash photolysis experiments. This protein, compared to sperm whale myoglobin, has a more pronounced kinetic structure, which allows a precise determination of the kinetic parameters. As a working hypothesis we consider a sequential kinetic scheme to describe the "major" states. But it should be understood that each macrostate consists of a multiplicity of substates (1, 4):

$$A \longleftarrow B \longleftrightarrow M \longleftrightarrow S + L. \qquad (7)$$
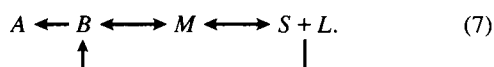
A denotes the bound state, B refers to the unrelaxed structure with the ligand confined to the heme pocket. M

denotes the ensemble of partially and fully relaxed structures, the ligand may be located either in the heme pocket or the protein matrix. $S + L$ describes external positions of the ligand ($L = CO$) in the solvent. By multiple flash photolysis experiments we probed whether the exchange between the substates is fast compared to transitions between the macrostates. In a double flash experiment an initial photolysing pulse is followed by a second one with a delay in time of τ. This allows us to monitor the kinetic behavior of the rebound fraction in comparison with the kinetics of the whole ensemble of protein molecules. If the ensemble is inhomogeneous, one performs a kinetic hole burning experiment, which selects a fast fraction. In the homogeneous case the rebound fraction displays the same kinetic behavior as the whole ensemble of protein molecules. The experiment thus discriminates between inhomogeneous and homogeneous nonexponential processes and allows a rigorous test of Eqs. 3–6.

2 MATERIALS AND METHODS

Samples were prepared from salt-free, lyophilized powder of horse and sperm whale myoglobin (Sigma Chemical Co., St. Louis, MO). The material was dissolved at a concentration of 3 mM in a solvent containing 75% glycerol-water (by volume) and 0.1 M phosphate buffer at pH 7. The protein solution, equilibrated with carbon monoxide at 1 at, was reduced by adding a 10-fold excess of $Na_2S_2O_4$ under unaerobic conditions. The sample cell consisted of two glass plates separated by a 100 microns teflon spacer. Alternatively, we used a 1 cm cell to exclude laser heating effects. The concentration was adjusted to give 1–1.5OD at 423 nm. The cell was mounted in a helium flow cryostat (Oxford), which allowed the control of temperature to an accuracy of 0.1 K. Photolysis was achieved using 3 and 8 ns pulses of a frequency doubled Nd:YAG Laser (532 nm, 120 mJ). Different pulse widths were employed to check for multiple photolysis during the laser pulse. The transient absorption change of the sample was monitored with the light of a stabilized tungsten lamp. A monochromator selected the desired wavelength, typically 436 nm. Laser stray light was removed using blue filters. A photomultiplier tube (Hamamtsu R928) coupled to a two-way amplifier system (100 and 1 MHz) recorded the kinetic response. Between 10 ns and 5 μs a digital oscilloscope (Techscope 2100, Gould) was used for data storage at a resolution of 8 bit. From 1.2 μs up to 300 s a home-built recorder, operating on a logarithmic time base, averaged and stored the digitized data at 12 bit resolution. Nonlinearities caused by PMT saturation and amplifier gains were reduced to below 0.2%. The systems allowed the recording of extinction changes over 10 decades in time with a dynamic range of 3.5 decades. In the double pulse experiment a second Marx-Bank with a variable quarz-stabilised delay time opened the Pockels cell for the second flash. With a delay time of 100 μs both pulse-energies were equal and photolysed the complete interaction volume (96%). In the multipulse experiment the repetition time (0.1 s) of the laser flash lamp was used. The baseline was averaged over 3 ms before the first shot. 1–256 shots were averaged in each measurement depending on the temperature.

3 RESULTS

(a) Single flash experiments

Fig. 1 shows typical rebinding curves at selected temperatures. In the range of 200 to 250 K three processes can be distinguished which are assigned to the decay of the in-
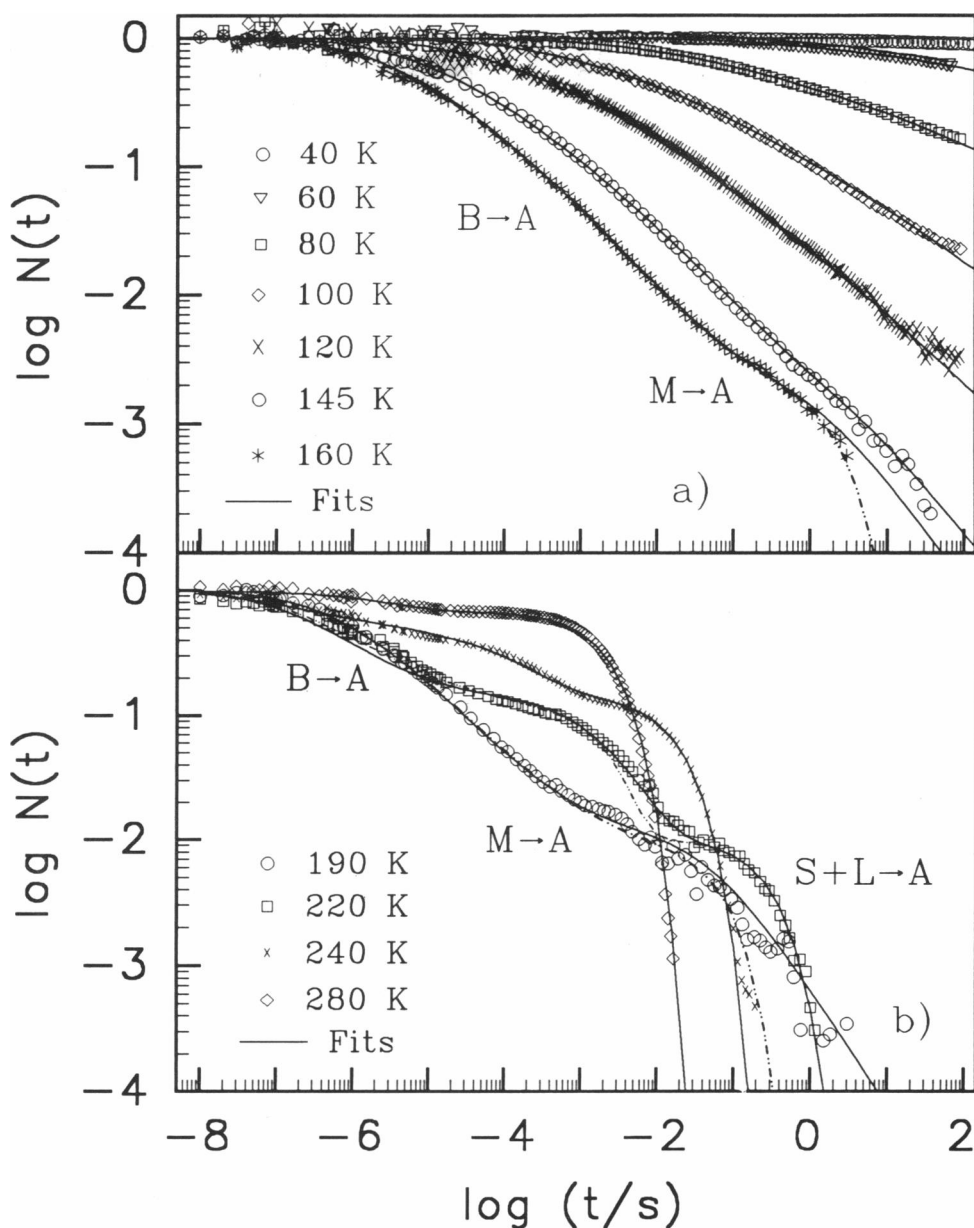
FIGURE 1 Survival fraction derived from single shot rebinding kinetics at (a) low temperatures, (b) intermediate and high temperatures. B, M, S + L indicate the decay of intermediate states according to Eq. 7, (——) fit to Eq. 6 and (– · ·–) to Eq. 3 complemented by an exponential process S + L → A.

termediate states $S + L$, M and B according to Eq. 7. As a first step the distribution of activation enthalpies $g(H_0)$ in the frozen structure is determined using $B \rightarrow A$ below 140 K. For parameterisation we employ the Gamma distribution of Young and Bowne (6). We obtain a preexponential in the Arrhenius law $A = 1.6 (\pm 0.6) \cdot 10^9 \cdot T/$ 100K s^{-1}, a peak enthalpy of 12.6 (± 0.5) kJ/mol and a width parameter $\alpha^{-1} = 1.2 (\pm 0.05)$ kJ/mol. These values are similar to what was found for sperm whale myoglobin (3). This result serves as input to fit the kinetics above 140 K by adjusting the parameters of Eqs. 3–6. Recombination from the solvent $S + L \rightarrow A$, which is

not covered by the models, was accounted for by an additional exponential process in the pseudo first order regime. Both models describe the data reasonably well, the homogeneous model (Eq. 3), however, does not reproduce the nonexponential shape of $M \rightarrow A$ (Fig. 1).

Fig. 2 a shows an Arrhenius plot of the structural relaxation times τ_c (Eqs. 3 and 6). Both models yield an activation energy of 44 (± 2) kJ/mol. The preexponential amounts to 10^{13} s^{-1} within a factor of three. Also the resulting β parameters (Fig. 2b) are nearly coincident. For both models we observe a step-like decrease in β above 200 K. It should be mentioned that the numbers
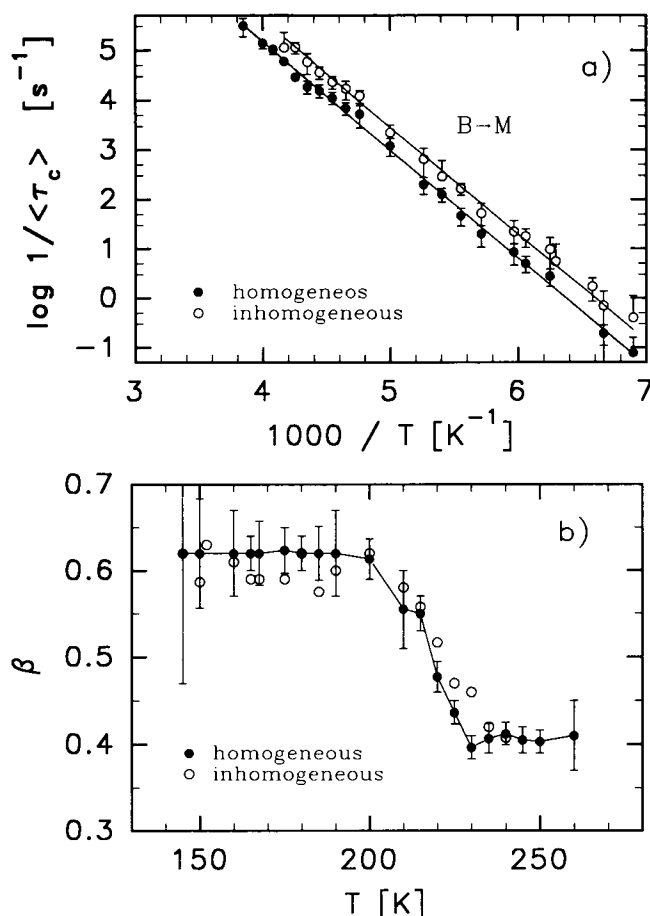
FIGURE 2 Parameters of the fits to single pulse rebinding curves according to the inhomogeneous and homogeneous model (Eqs. 3 and 6, respectively) (a) inverse mean structural relaxation time τ_c vs. inverse temperature, (b) stretching parameter β vs. temperature.

given above depend on solvent composition, as will be discussed elsewhere.

Fig. 3 compares the enthalpy shifts. The homogeneous model yields $H_f = 30.5$ (± 1) kJ/mol, which is approximately consistent with the prediction of Agmon and Hopfield (2). The slight decrease in H_f above 220 K most likely originates from the escape of CO to the solvent, $M \to S + L$ in addition to direct recombination $M \to A$ (Fig. 1b). The inhomogeneous model in contrast yields a strongly temperature dependent activation energy. This result is not compatible with Eq. 6, which predicts a fixed energy shift ΔH. One may conclude that the shape of the enthalpy distribution changes during structural relaxation. Further insight can be obtained by multiple excitation experiments.

(b) Double and multiple excitation experiments

We first consider a double pulse experiment. Mathematically, the resulting rebinding curve after the second flash can be written as

$$N^{(2)}(t) = N^{(1)}(\tau + t) + (1 - N^{(1)}(\tau)) \cdot N^*(t), \quad (8)$$

where $N^{(1)}(t)$ denotes the single pulse kinetics and $N^*(t)$ refers to the kinetics of the rebound fraction. In the trivial case of exponential kinetics the first and last term on the r.h.s. in Eq. 8 cancel, leaving $N^{(2)}(t) = N^{(1)}(t)$, otherwise $N^{(2)}(t) > N^{(1)}(t)$. $N^*(t)$ can be extracted from the data by inverting Eq. 8:

$$N^*(t) = \frac{N^{(2)}(t) - N^{(1)}(\tau + t)}{1 - N^{(1)}(\tau)}. \quad (9)$$

If the system is inhomogeneous, the selected molecules retain their high rebinding rates making $N^*(t)$ decay faster than $N^{(1)}(t)$, whereas in the homogeneous case, the rebound fraction behaves like the whole ensemble, leading to $N^*(t) = N^{(1)}(t)$. In the inhomogeneous case, Eq. 8 has been evaluated for each individual rate k, and an average is performed over a rate distribution $g(k)$:

$$N^{(2)}_{inh}(t) = \langle N^{(2)}_k(t) \rangle_{g(k)}. \quad (10)$$

If $N^{(1)}_k(t)$ decays exponentially, $N^{(2)}_k(t)$ equals $N^{(1)}_k(t)$ and one obtains:

$$N^{(2)}_{inh}(t) = N^{(1)}_{inh}(t). \quad (11)$$

In the multipulse case, Eqs. 8–11 have to be iterated $n - 1$ times (for n pulses). Figs. 4, a and b, show the double pulse kinetics at 145 K with delay times of 10^{-4} and 10^{-1} s, respectively. Depicted are the measured single ($N^{(1)}(t)$) and double ($N^{(2)}(t)$) shot rebinding curves together with the calculated kinetics of the rebound fraction $N^*(t)$ (Eq. 9) and the prediction of the inhomogeneous model. For a delay time of 10^{-4} s $N^{(2)}(t)$ equals $N^{(1)}(t)$ and $N^*(t)$ follows the predicted curve. These facts imply that process $B \to A$ indeed consists of
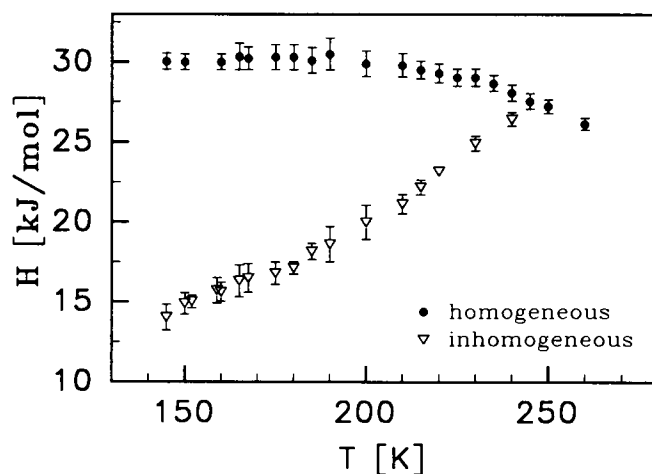

FIGURE 3 Final enthalpy barrier H_f of the homogeneous model and peak position $H_0 + \Delta H$ of the shifted enthalpy distribution (inhomogeneous model) vs. temperature.
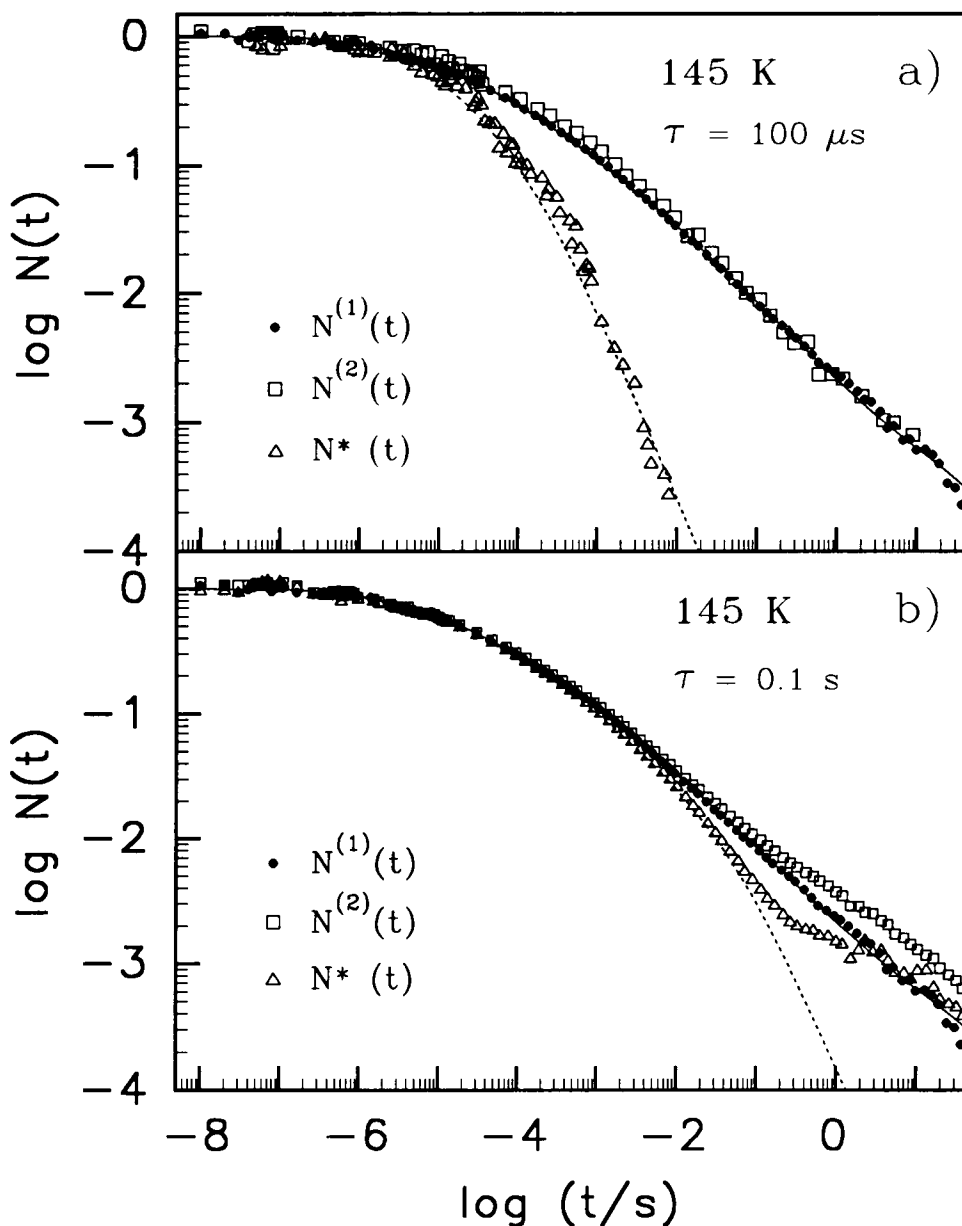
FIGURE 4   Single ($N^1(t)$) and double ($N^2(t)$) pulse kinetics at 145 K and the calculated kinetics of rebound fraction $N^*(t)$ (Eq. 9) together with the fit to the single pulse data (———) and the prediction of the inhomogeneous model (- - -) for $N^*(t)$. The delay times are (a) 10^{-4} s and (b) 10^{-1} s.

an inhomogeneous superposition of exponentially re-binding molecules (Eqs. 10, 11). The situation changes at 10^{-1} s (Fig. 4 b), where the just barely visible shifted process $M \rightarrow A$ can be significantly enhanced by apply-ing the second laser pulse. Such behavior would be ex-pected for a homogeneous nonexponential process and indeed the calculated $N^*(t)$ deviates drastically from the prediction of the inhomogeneous model. This finding is confirmed by the measurements at 185 K (Figs. 5 and 6). For $\tau = 10^{-4}$ s (Fig. 5 a) the kinetics of the rebound fraction $N^*(t)$ lies in between the inhomogeneous pre-diction and the completely homogeneous case. The sec-ond process ($M \rightarrow A$) shows a greatly reduced amplitude

but is only barely faster than that in $N^{(1)}(t)$. Subtracting this process from both kinetics (Fig. 5 b) shows that pro-cess $B \rightarrow A$ is still inhomogeneous i.e. follows the pre-dicted curve. For a delay time of 10^{-1} s, we probed the second process, $M \rightarrow A$, (Fig. 6 a). In that case $N^*(t)$ follows $N^{(1)}(t)$ closely. This result implies homogeneous recombination in spite of the nonexponential kinetic shape. Fits of $M \rightarrow A$ by a stretched exponential function yield an exponent of $\beta_M = 0.45$ (± 0.05).

A more rigorous test of the degree of homogeneity is achieved by multiple excitation experiments shown in Fig. 6 b. Process $M \rightarrow A$ increases in magnitude due to repetitive pumping, but also slows down with increasing
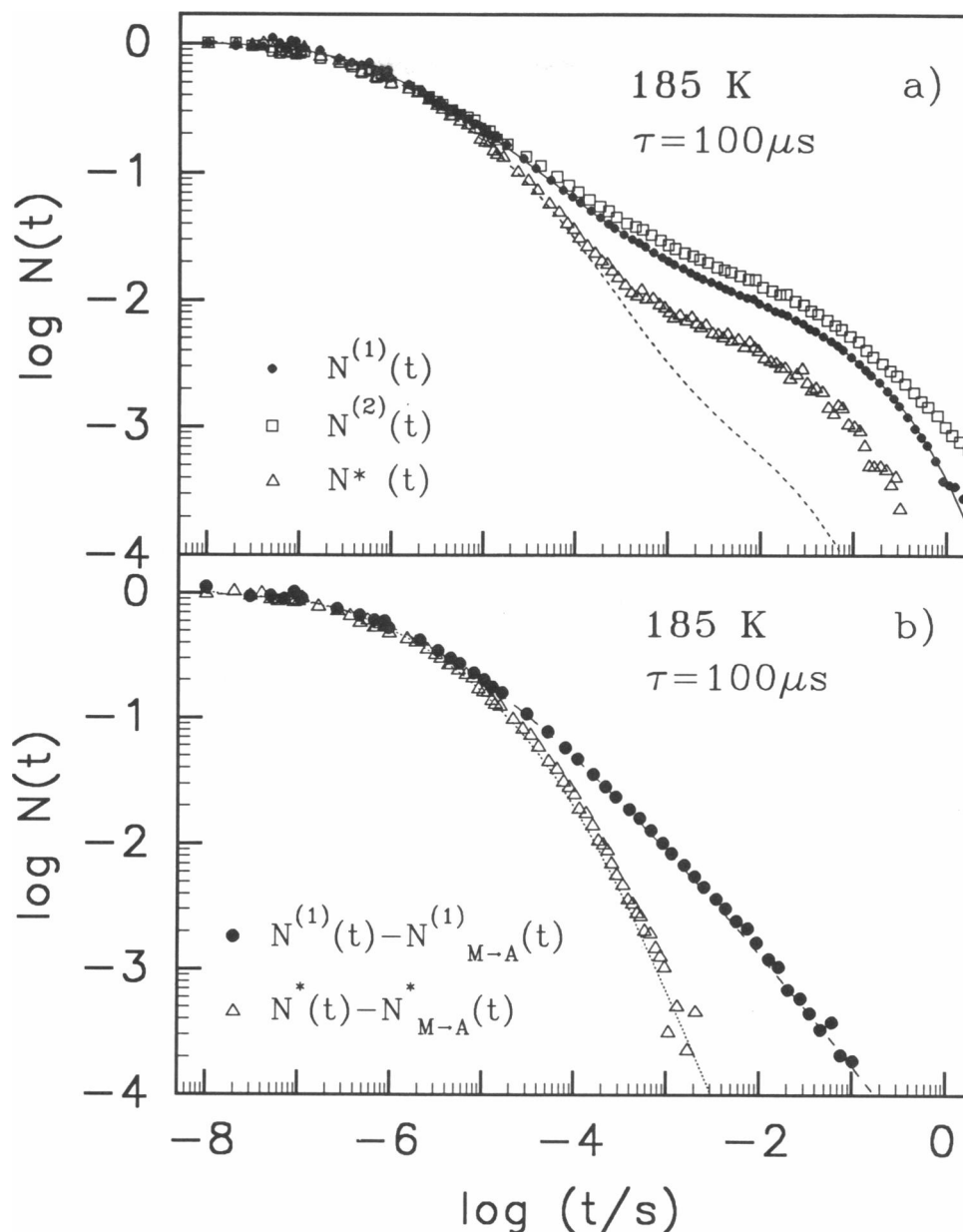
FIGURE 5 (*a*) As in Fig. 4 but at $T = 185$ K with a delay time of $10 \, \text{s}^{-4}$. (*b*) $N^1(t)$ and $N^*(t)$ after subtraction of process $M \to A$. Dashed and dotted lines correspond to the inhomogeneous model.

number of shots. Starting from the single pulse result the rebinding curve for a given number of pulses is calculated by iterating Eq. 8 with $N^*(t) = N^{(1)}(t)$, i.e., under the assumption of homogeneity. The result of this procedure is given by the solid lines in Fig. 6 *b* and shows excellent agreement with the data. However an additional process, not observable in the single pulse measurement becomes visible for $n \geq 20$, which is accounted for by adding another component to $N^{(1)}(t)$ and varying its parameters until the multipulse extrapolation fits the data.

We succeeded to separate both components by converting the kinetics to an activation energy spectrum. At

first we calculate an approximate rate distribution $g(k)$ using the time derivative of the fits to the data (7)

$$k \cdot g(k) \approx -N(t) \frac{d \log (N(t))}{d \log (t)}. \quad (12)$$

$g(k)$ is then transformed to $g(H)$ by

$$-g(k)dk = g(H)dH \quad (13)$$

using the Arrhenius law and the preexponential of ($B \to A$) given above. Fig. 7 *a* shows the result of the single flash data, which is discussed in more detail below. Fig. 7 *b* displays a magnified version of the single and multi-
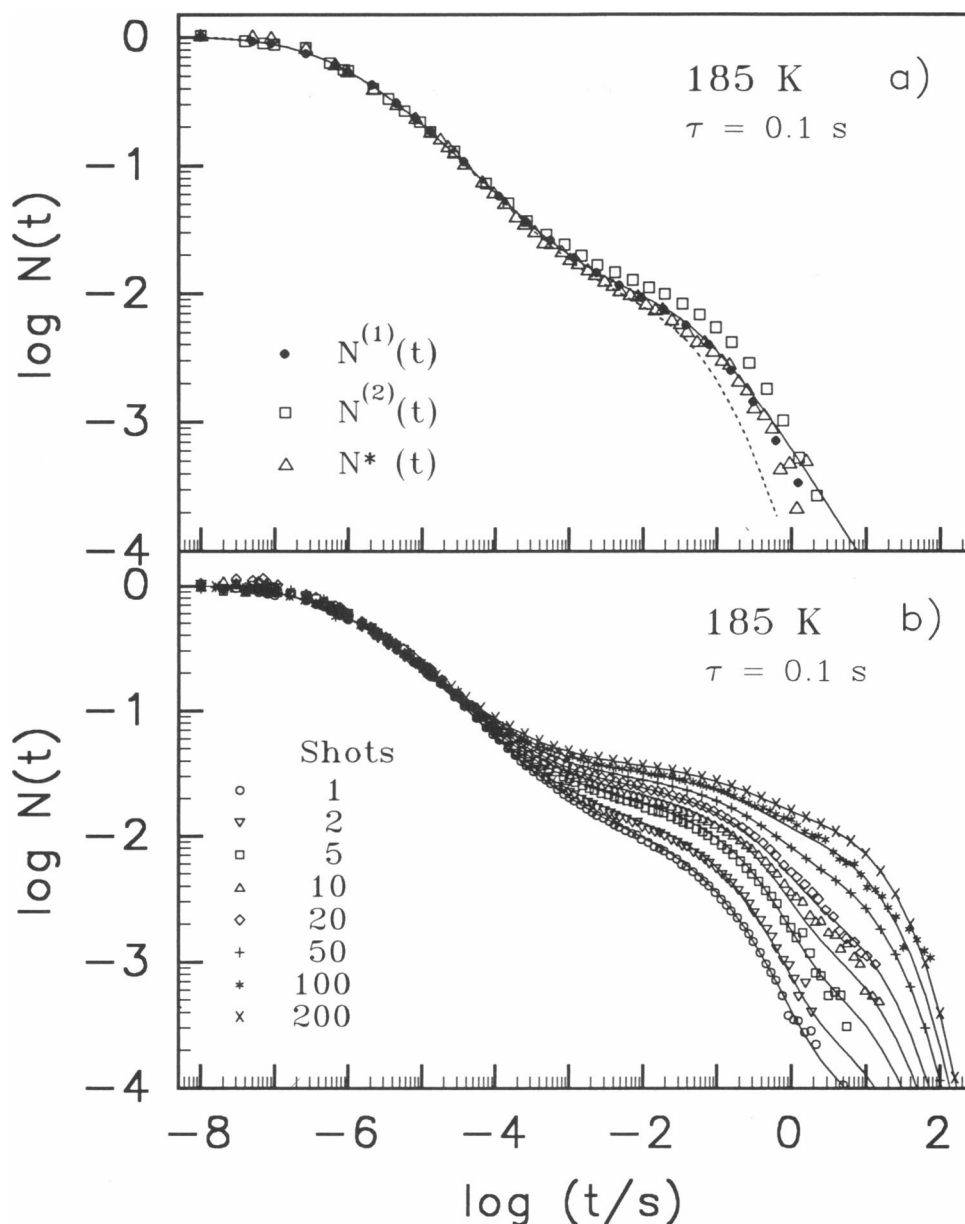
FIGURE 6 (*a*) As in Fig. 5 at T = 185 K, delay time 10^{-1} s (*b*) Multiple excitation at T = 185, delay time 10^{-1} s. The continuous lines represent the extrapolation from the single pulse result under the assumption of complete homogeneity of the sample.

pulse spectrum at 185 K. The comparison shows that the intermediate M is increasingly populated with the number of shots. Also its peak activation enthalpy increases. Further the additional process, which occurs for $n \geq 20$, has the activation energy of $(S + L \rightarrow A)$, observed in single flash experiments at higher temperatures (Fig. 7 *a*). Thus pumping of CO to the solvent occurs, contributing to the slowing down of $N^n(t)$, but the main effect is due to the homogeneous intermediate M.

We further consider the question of how fast the relaxed deoxy structure is converted back to the ligated conformation. In the data analysis above, instantaneous back relaxation upon rebinding was assumed. In order to

test the influence of a finite relaxation time, two possibilities were considered: first, the barrier begins to relax at the instant of rebinding with a rate equal to the off-relaxation rate τ_c. Second, the barrier remains at the value it has after recombination but is allowed to relax further after the next laser flash. In Fig. 8 these different possibilities are shown to improve the predictions of the inhomogeneous model in the crossover time range, but they cannot explain the data at longer times.

We emphasize an inherent difficulty in testing the above models, where all changes are assumed to occur in the photolysed state, by multiple excitation experiments: One looks specifically at the behavior of the rebound
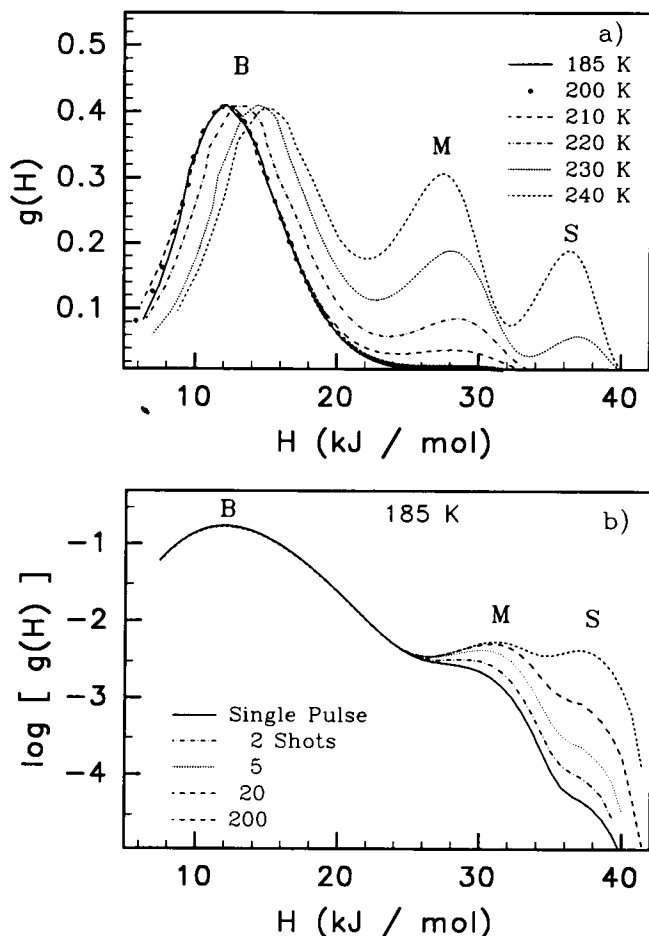
FIGURE 7 (a) Enthalpy distribution of the recombination kinetics at high temperatures (Eqs. 12 and 13) normalized to peak height of B. (b) Enthalpy distribution of the recombination kinetics of multiple pulse excitation at 185 K. The actual activation energy for the solvent process is 53 kJ/mol. The apparent value of 37 kJ/mol in the plot is due to the preexponential of process $B \to A$, which was used for the whole data set of a given temperature for the conversion of rate to energy.

FIGURE 8 (●) $N^2(t)$ at 160 K (delay: 10^{-1} s), (——) $N^1(t)$ single pulse fit, (— · — · —) $N^2(t)$ inhomogeneous prediction assuming instantaneous back-relaxation, (· · · · ·) $N^2(t)$ back-relaxation after rebinding with τ_c and (— · · — · · —) $N^2(t)$ no back-relaxation (see text for details).

together with the prediction of $g(H_0)$ represented by the lines. The prediction is excellent up to 200 K, above however, the initial phase $B \to A$ does not speed up with increasing temperature as should be expected. Converting the kinetics to an enthalpy spectrum (Fig. 7 a), an up shift of the B distribution appears starting at 210 K. Thus we observe an additional relaxation process now supporting the inhomogeneous model.

4 DISCUSSION AND CONCLUSION

Multiple flash photolysis experiments on sperm whale myoglobin were originally performed at low temperatures (70 K) with delay times of a few seconds (1). Since

fraction. These molecules have a history of recombination which is not included in the models. For an inhomogeneous result the answer is definite. But apparent homogeneity may arise from equilibration by rebinding after the first pulse. Since we observe two processes of different character we can exclude equilibration by release of the binding energy or back-relaxation.

These results, homogeneity of the M decay and $H_f = 30.5$ (± 1) kJ/mol support the model of Agmon and Hopfield (2), although the nonexponential decay of M (Fig. 1 b, 240 K, dashed line) is not reproduced. However, in order to fit the data, we had to accept a step-like decrease in the parameter β above 200 K (Fig. 2 b), indicating a change in shape of the relaxation time distribution. A more detailed inspection revealed instead an anomaly concerning the initial phase $B \to A$. Fig. 9 shows the data in the temperature range between 200 K and 240 K (after subtraction of $S + L \to A$ and $M \to A$)
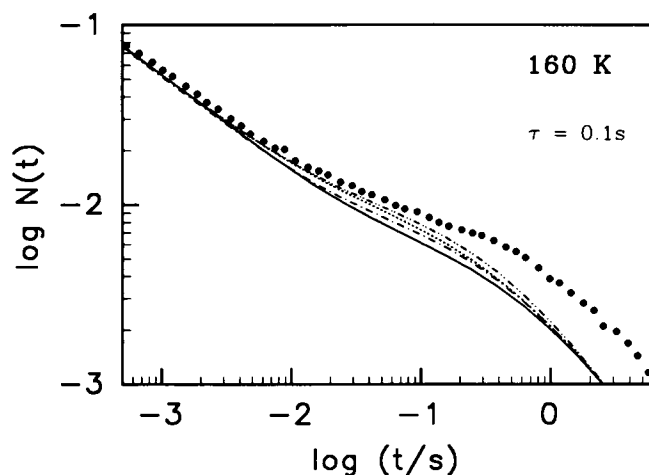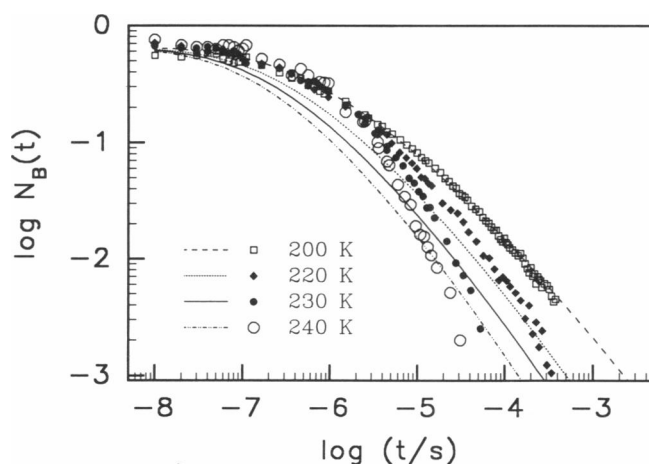

FIGURE 9 Survival fraction of single shot rebinding kinetics at high temperatures after subtraction of the processes $M \to A$ and $S + L \to A$ compared with the extrapolation based on the low temperature barrier distribution (Eq. 1).
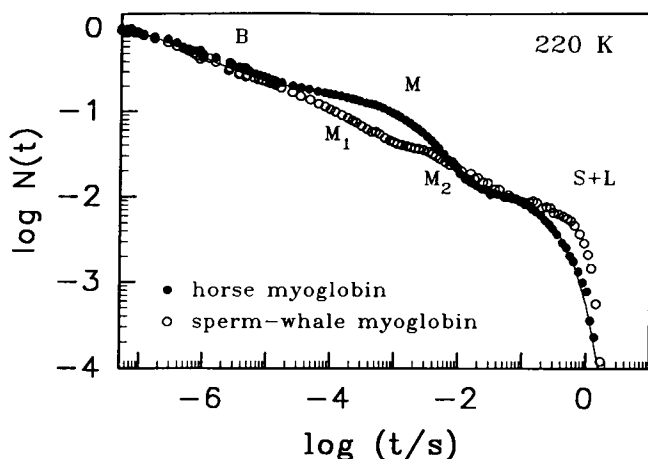
FIGURE 10 Single pulse kinetics of horse and sperm whale myoglobin at 220 K.

the kinetic amplitude did not decrease with the number of shots, these experiments proved the nonequivalence of individual protein molecules. A discussion that relates this result to the concept of conformational substates is given in Frauenfelder et al. (8). However, EXAFS and optical experiments (9–11) showed that, after extended continuous illumination of sw MbCO with white light, pumping to long lived states occurs at low temperatures. For horse myoglobin we observe pumping above 90 K, which could indicate a slight shift in the energy distribution $g(H_0)$ or restricted structural diffusion (12). However, above 140 K a distinct new process $M \rightarrow A$ appears at long times whose amplitude and characteristic time can be enhanced by multiple excitation (Fig. 4 b). Finally, above 180 K pumping of CO to the solvent can be observed by multiple excitation (Fig. 6 b).

Our experiments exclude the inhomogeneous model (Eq. 6) as far as intermediate M is concerned. However the apparent temperature independence of $B \rightarrow A$ above 210 K does support an upshift in the enthalpy distribution as predicted by the inhomogeneous model. This feature is also apparent in the sperm whale case (see Fig. 11 of reference 3). Fig. 10 compares horse and sperm whale myoglobin at 220 K. A more detailed comparison will be published elsewhere. The initial "temperature independent" phases are almost identical. However, instead of a single intermediate phase M, sperm whale myoglobin shows two components M_1, M_2. The resulting strongly stretched kinetics was the main reason for the successful fit to the inhomogeneous model in reference 3. In our view, the anomaly resides in the "temperature independent" initial decay of B. Apart from an enthalpy shift one could equivalently consider an entropy increase, according to the following argument:

The mean square displacement of the heme iron, derived from Mössbauer spectroscopy, shows a nonlinear enhancement starting at 200 K (13). Thus, above this

temperature, anharmonic motions of the heme become faster than the nuclear life time of 10^{-7} s. This effect enlarges the phase space of deoxyheme accessible within the life time of B ($5 \cdot 10^{-6}$ s) relative to the more rigid bound state.

To study the degree of homogeneity of $B \rightarrow A$, we performed double pulse experiments at 220 K using a delay of 100 μs. As a result, we obtain a slightly larger yield of $B \rightarrow A$ than expected for a homogeneous situation. Recently, Tian et al. (14) performed double pulse experiments on sperm whale myoglobin above 260 K with delays as short as 80 ns. They also obtain an enhanced geminate yield in particular at low pH. The pH dependence suggests that the bound state conformations, A_0 and A_1, which differ in activation energy, are not rapidly exchanging (10). Tian et al. (14) could further demonstrate the homogeneity of ligand escape to the solvent.

According to their analysis, the barrier at the heme which controls ligand binding at physiological temperatures amounts to 18 kJ/mol. A similar result was obtained by Steinbach et al. (3). These findings raise the question whether in the case of horse myoglobin it is the barrier of M (30 kJ/mol) or B (15 kJ/mol) which controls the final binding step.

At physiological temperatures more than 95% of the ligands reach the solvent after photolysis. Under these conditions ligand binding proceeds with a fast preequilibrium between solvent and heme pocket in sequence with the reaction at the heme. The on-rate can be written as (4):

$$\lambda_{on} \approx k_H \cdot P. \tag{14}$$

k_H represents the fluctuationally averaged recombination rate with the heme and P denotes the heme pocket occupation factor. For λ_{on} we derive an activation energy of 12 (± 2) kJ/mol comparable with the sperm whale result (3, 4). Thus, if M would be the geminate pair state, one had to assume that CO binds in the pocket by 18 kJ/mol to compensate for the 30 kJ/mol of the M barrier. This seems unlikely for a weakly polar molecule. A more likely candidate is the B state leading to weak binding, 3 kJ/mol, in the pocket. This value could even be smaller if the change in the B barrier above 200 K is purely entropic. Furthermore, since the barriers of B and M have approximately the same preexponentials (10^9 s^{-1}) but differ drastically in height, one can discard M as a relevant intermediate of the recombination process from the solvent. Consequently one has to consider the direct access ($S + L \rightarrow B$), which is shown by the dashed line in Eq. 7.

Transient infrared experiments on horse myoglobin, probing the C—O stretching band in the bound (A) and the photolyzed (B) states (15), reveal that above 200 K the B bands decay faster than the growth of the A state

population. According to this result the ligand in M may have moved out of the heme pocket. A related possibility could be dynamic averaging of the B bands by structural fluctuations. Recently the homogeneous model was extended by explicitly treating ligand and structural displacements on a two-dimensional energy surface (16). This certainly represents a step towards a more realistic description.

To summarize, neither of the two proposed models can entirely explain the data. Two distinct relaxation processes are observed, which involve an upshift in the activation energy spectrum. The first, leading to M, may reflect fluctuations of the protein matrix and ligand transport, while the second may be related specifically to the flexibility of the heme.

A unifying model should account for differences observed between various ligands (CO, O_2, NO), myoglobin species as well as for the absence of intermediate M in some proteins (3, 17–19).

REFERENCES

1. Austin, R. H., K. W. Beeson, L. Eisenstein, H. Frauenfelder, and I. C. Gunsalus. 1975. Dynamics of ligand binding to myoglobin. *Biochemistry.* 14:5355–5373.

2. Agmon, N., and J. J. Hopfield. 1983. CO binding to heme proteins. *J. Chem. Phys.* 79:2042–2053.

3. Steinbach, P. J., A. Ansari, J. Berendzen, D. Braunstein, K. Chu, B. R. Cowen, D. Ehrenstein, H. Frauenfelder, J. B. J. Johnson, D. C. Lamb, S. Luck, J. R. Mourant, G. U. Nienhaus, P. Ormos, R. Philipp, A. Xie, and R. D. Young. 1991. Ligand binding to heme proteins: connection between dynamics and function. *Biochemistry.* 30:3988–4001.

4. Doster, W., D. Beece, S. F. Bowne, E. E. Di Iorio, L. Eisenstein, H. Frauenfelder, L. Reinisch, E. Shyamsunder, K. H. Winterhalter, and K. T. Yue. 1982. Control and pH dependence of ligand binding to heme proteins. *Biochemistry.* 21:4831–4839.

5. Šrajer, V., L. Reinisch, and P. M. Champion. 1988. Protein fluctuations, distributed coupling, and the binding of ligands to heme proteins. *J. Am. Chem. Soc.* 110:6656–6670.

6. Young, R. D., and S. F. Bowne. 1984. Conformational substates and barrier height distributions in ligand binding to heme proteins. *J. Chem. Phys.* 81:3730–3737.

7. Steinbach, P. J., K. Chu, H. Frauenfelder, J. B. Johnson, D. C. Lamb, G. U. Nienhaus, T. B. Sauke, and R. D. Young. 1992. Determination of rate distribution from kinetic experiments. *Biophys. J.* 61:235–245.

8. H. Frauenfelder, F. Parak, and R. Young. 1988. Conformational substates in proteins. *Annu. Rev. Biophys. Biophys. Chem.* 17:451–479.

9. Powers, L., J. L. Sessler, G. L. Woolery, and B. Chance. 1984. CO bond angle changes in photolysis of carboxymyoglobin. *Biochemistry.* 23:5519.

10. Ansari, A., J. Berendzen, D. Braunstein, B. R. Cowen, H. Frauenfelder, M. K. Hong, I. E. T. Iben, J. B. Johnson, P. Ormos, T. B. Sauke, R. Scholl, A. Schulte, P. J. Steinbach, J. Vittitow, and R. D. Young. 1987. Rebinding and relaxation in the myoglobin pocket. *Biophys. Chem.* 26:337–355.

11. Šrajer, V., L. Reinisch, and P. M. Champion. 1991. Investigation of laser-induced long-lived states of photolyzed MbCO. *Biochemistry.* 30:4886–4895.

12. Doster, W., Ch. Holzhey, H. Miesmer, and F. Post. 1990. The effect of heterogeneous structural diffusion on ligand binding to heme proteins. *J. Biol. Phys.* 17:281–295.

13. Keller H., and P. G. Debrunner. 1980. Evidence for conformational and diffusional mean square displacements in frozen aqueous solution of oxymyoglobin. *Phys. Rev. Lett.* 45:68–71.

14. Tian, W. D., J. T. Sage, V. Šrajer, and P. M. Champion. 1992. Relaxation dynamics of myoglobin in solution. *Phys. Rev. Lett.* 68:408–411.

15. Hong, K., E. Shyamsunder, R. H. Austin, B. S. Gerstman, and S. S. Chan. 1991. Time-resolved infrared studies of molecular diffusion in myoglobin. *Phys. Rev. Let.* 66:2673–2676.

16. Agmon, N., and S. Rabinovich. 1992. Diffusive dynamics on potential energy surfaces: Nonequilibrium CO binding to heme proteins. *J. Chem. Phys.* 97:7271–7286.

17. Di Iorio, E. E., U. R. Hiltpold, D. Filipovic, K. H. Winterhalter, E. Gratton, E. Vitrano, A. Cupane, M. Leone, and L. Cordone. 1991. Protein Dynamics. *Biophys. J.* 59:742–754.

18. Doster, W., S. Bowne, H. Frauenfelder, L. Reinisch, and E. Shyamsunder. 1987. Recombination of CO to ferrous horse radish peroxidase types A and C. *J. Mol. Biol.* 194:299–312.

19. Ehrenstein, D., and G. U. Nienhaus. 1992. Conformational substates in azurin. *Proc. Natl. Acad. Sci. USA.* 89:9681–9685.